

## Nanosized mixed aggregates of alkylated *p*-sulfonatocalix[*n*]arenes and cetyltrimethylammonium bromide: self-organization and catalytic activity

I. S. Ryzhkina,<sup>a\*</sup> Yu. V. Kiseleva,<sup>a</sup> L. I. Murtazina,<sup>a</sup> Yu. N. Valitova,<sup>b</sup> S. E. Solov'eva,<sup>a</sup>  
L. M. Pilishkina,<sup>a</sup> and A. I. Konovalov<sup>a</sup>

<sup>a</sup>A. E. Arbuzov Institute of Organic and Physical Chemistry,  
Kazan Research Center of the Russian Academy of Sciences,  
8 ul. Akad. Arbuzova, 420088 Kazan, Russian Federation.  
Fax: +7 (843) 275 2253. E-mail: ryzhkina@iopc.kcn.ru

<sup>b</sup>Kazan Institute of Biophysics and Biochemistry,  
Kazan Research Center of the Russian Academy of Sciences,  
2/31 ul. Lobachevskogo, 420111 Kazan, Russian Federation

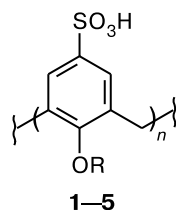
Self-organization and catalytic activity of supramolecular systems based on a series of *O*-alkylated *p*-sulfonatocalix[*n*]arenes (SCA: *n* = 4, 6, 8; R = Bu, Oct, Dod (Oct is octyl, Dod is dodecyl)) and cetyltrimethylammonium bromide (CTAB) were studied by dynamic light scattering, tensimetry, and spectrophotometry. In aqueous solutions containing SCA ( $10^{-6}$ – $10^{-4}$  mol L<sup>-1</sup>) and CTAB ( $10^{-2}$ – $10^{-12}$  mol L<sup>-1</sup>), mixed associates and SCA–CTAB micelles are formed in a wide concentration range. Their sizes (100–300 nm), properties, and reactivity depend mainly on the structure and concentration of the starting components, as well as on the nature of their associates in solutions. A relationship between the nonlinear concentration dependences of the sizes of SCA–CTAB micelles (SCA: *n* = 4, 6, 8; R = Dod) and their catalytic activity in the hydrolysis of *O*-ethyl *O*-(4-nitrophenyl) chloromethylphosphonate was established. The study of the physiological effect on plant cells in solutions of SCA (*n* = 6; R = Dod), CTAB, and their mixtures showed that SCA and CTAB exerted opposite effects on the energy exchange in the wheat root cells, while a mixed solution of these substances (1 : 1) has almost no effect on the physiological state of the roots, which is due to the formation of stable CTAB–SCA aggregates that protect the biosystem from the action of the starting components.

**Key words:** alkylated *p*-sulfonatocalix[*n*]arenes, cetyltrimethylammonium bromide, nanosized aggregates, supramolecular systems, catalytic activity, hydrolysis, *O*-ethyl *O*-(4-nitrophenyl) chloromethylphosphonate, physiological effect, wheat root cells, energy exchange.

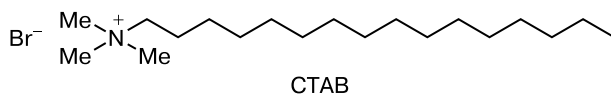
Calixarenes are synthetically accessible complicatedly organized three-dimensional macrocyclic phenols with a large surface containing hydrophilic functional groups and hydrophobic regions, *i.e.*, these are amphiphilic molecules prone to spontaneous association with the transition to the pseudo-microheterogeneous micellar phase analogous to traditional surfactants.<sup>1–3</sup> Accessible functionalization of calixarenes, which makes it possible to control their physicochemical properties by changing the nature of substituents and the number of aromatic rings, and their ability to form supramolecular complexes with cations, anions, and neutral molecules due to the hydrophobic cavity, result in permanently increasing scientific interest in compounds of this class. This is due to the possibility to use them in both fundamental and applied studies.<sup>1–3</sup> From the view-

point of practical use, *p*-sulfonatocalix[*n*]arenes (SCA: *n* = 4, 6, 8) and their derivatives are among most promising compounds.<sup>1–7</sup> The predominant majority of publications are devoted to the properties of non-modified *p*-sulfonatocalix[*n*]arenes, which, being host molecules, form supramolecular complexes with diverse inorganic and organic compounds.<sup>4,5</sup> The properties of SCA modified by alkyl substituents are insufficiently studied<sup>1–3</sup>; the question about sizes of SCA aggregates (micelles) has not yet been considered. We systematically studied the micelle formation of alkylated SCA **1–5** (*n* = 4, 6, 8; R = Bu, Oct, Dod (Oct is octyl, Dod is dodecyl)) and revealed specific features of this process characteristic of SCA. In particular, it was shown that in aqueous solutions of these compounds in the range of critical micelle concentration (CMC) nanoparticles of the micelle

type are formed with the effective hydrodynamic diameter  $\sim 200$  nm.<sup>8</sup>



	<i>n</i>	R		<i>n</i>	R
<b>1</b>	4	Bu	<b>4</b>	6	Dod
<b>2</b>	4	Oct	<b>5</b>	8	Dod
<b>3</b>	4	Dod			



The structure of SCA assumes a possibility of strong and selective binding with organic compounds capable of formation of host–guest complexes, first of all, due to electrostatic interactions of negatively charged functional groups, which are located at the upper and lower "rims" of the hydrophobic cavity formed by the aromatic fragments.<sup>1–6</sup> The interaction of SCA with various biologically important nitrogen-containing organic substances, including ammonium salts, has been studied in rather detail.<sup>1–6</sup> However, a few works are devoted to the study of binding of non-modified SCA with alkylated ammonium compounds, which are well known as cationic surfactants,<sup>9</sup> whereas the interaction of alkylated SCA derivatives with cationic surfactants remain almost unstudied. At the same time, cationic surfactants, particularly, cetyltrimethylammonium bromide (CTAB), chosen for studying mixed supramolecular systems with alkylated SCA possess several important properties and a widely and long ago have been used in fundamental studies and industrial technologies as detergents, bactericidal preparations, micellar catalysts, modifiers of water-soluble polymers of synthetic and natural origin, *etc.*<sup>10–13</sup> We have previously shown that in mixed supramolecular systems based on amphiphilic functionalized calix[4]resorcinarenes and cationic or nonionic surfactants the CMC decrease considerably compared to individual surfactants. At low concentrations of amphiphilic functionalized calix[4]resorcinarenes in solutions of calixarene–surfactant mixtures, nanoparticles are formed, which efficiently bind phosphorus acid esters and catalyze their cleavage under mild conditions with an increased rate. This makes it possible to consider supramolecular systems based on amphiphilic functionalized calix[4]resorcinarenes as biomimetic catalytic systems, and amphiphilic functionalized calix[4]resorcinarenes can be considered as substances potentially capable of operating as auxiliary components in various surfactant compositions.<sup>14–17</sup> Therefore, the detailed study of the aggrega-

tion behavior and catalytic activity of supramolecular systems based on amphiphilic calixarenes of various structure and surfactants is of significant interest from both theoretical and practical points of view.

The purpose of the present work is to study the self-organization of mixed solutions of amphiphilic *p*-sulfonatocalix[*n*]arenes **1–5** and cetyltrimethylammonium bromide and catalytic activity of the supramolecular systems based on these compounds in the hydrolysis of *O*-ethyl *O*-(4-nitrophenyl) chloromethylphosphonate (ENCP) and to reveal the effect of solutions of SCA, CTAB, and their mixtures on the energy exchange in wheat root cells.

## Experimental

The SCA studied were synthesized according to earlier described procedures.<sup>18–20</sup> The parameters of the IR and <sup>1</sup>H NMR spectra of compounds **1–5** corresponded to the above presented literature data. The surface activity of SCA, CTAB, and SCA–CTAB systems were studied, recording the surface tension ( $\sigma$ ) isotherms in water–air systems by the du Nouy ring detachment method (Sigma 702ET high-precision tensiometer equipped with a temperature-maintained jacket); the pH of solution was determined with an I-160 ion meter. The size of associates (effective hydrodynamic diameter (*D*) of kinetically mobile particle at the maximum of the distribution curve) was determined by the light scattering method on a FotoCor Complex photon correlation spectrometer for dynamic and static light scattering and on a Malvern Instruments Zetasizer Nano ZS high-sensitive analyzer. The procedure of sample preparation for studies of the particle size provided necessary "dust-removal" of solutions (use of disposable pipettes, cells with caps in the instrumental assembly, and disposable filters 0.45  $\mu$ m, Millex HN). The measurement of sizes of nanoassociates in solutions was preceded by the control study of freshly prepared bidistilled water, which was used for the preparation of solutions, only if the analyzer detected the complete absence of any particles. Experiments were carried out with temperature maintained constant at  $25 \pm 0.1$  °C. The plots  $\sigma = f(C_{\text{CTAB}})$  and  $D = f(C_{\text{CTAB}})$  in the absence and in the presence of SCA **1–5** were studied in the range of CTAB concentrations from  $1 \cdot 10^{-18}$  to  $1 \cdot 10^{-2}$  mol L<sup>-1</sup>. The relative measurement errors for the particle size and surface tension of solutions calculated by the results of three independent measurements were 5–10% and 1–2%, respectively. The SCA concentrations in a mixture with CTAB usually were  $1.0 \cdot 10^{-4}$  mol L<sup>-1</sup>, whereas in the case of SCA **3** and **4** they varied from  $5.0 \cdot 10^{-6}$  to  $2.5 \cdot 10^{-4}$  mol L<sup>-1</sup>. Aqueous solutions of CTAB and SCA were prepared by the method of serial dilutions from the initial solutions with the concentration of substances  $1.0 \cdot 10^{-2}$  mol L<sup>-1</sup>.

The kinetics of hydrolysis of the ENCP substrate was studied spectrophotometrically under the pseudo-first-order reaction conditions (with respect to the formation of *p*-nitrophenolate,  $\lambda = 400$  nm) on a Perkin–Elmer Lambda 35 spectrophotometer at 25 °C, pH 8. The apparent (observed) reaction rate constants ( $k_{\text{app}}$ ) were determined by the first-order equation. Using the data of the concentration dependences of  $k_{\text{app}}$ , the binding constants ( $K_b$ ) of the substrates by the formed aggregates, the critical

micelle concentrations (CMC), and the rate constants of the reaction in the micellar pseudophase ( $k_m$ ) were calculated. For this purpose, we used the equation<sup>11</sup> for the calculation of the kinetic curves taking into account the substrate distribution between the volume and micellar phases

$$k_{\text{app}} = \frac{k_{\text{H}_2\text{O}} + k_m K_b C_{\text{Surf}}}{1 + K_b C_{\text{Surf}}}, \quad (1)$$

where  $k_{\text{H}_2\text{O}}/\text{s}^{-1}$  is the reaction rate constant in water,  $k_m/\text{s}^{-1}$  is the reaction rate constant in the micellar pseudophase, and  $C_{\text{Surf}}/\text{mol L}^{-1}$  is the surfactant (CTAB) concentration corrected to the CMC.

The object of the studies in biological experiments was spring wheat of the Lyuba sort (*Triticum aestivum* L.). In experiments, acrospires were grown on distilled water for 4 days.<sup>21</sup> Immediately after cutting, the roots of the wheat acrospires were placed into the working solutions and incubated in the Warburg apparatus.<sup>21</sup> The isolation and absorption of potassium ions by the root cells were judged about from a change in the content K in the incubation medium. The measurements were carried out on a PFM flame photometer. Preliminarily the roots were incubated in Warburg vessels, which made it possible to simultaneously detect the consumption of oxygen by the cells.

## Results and Discussion

The study of the effect of SCA 1–3 ( $n = 4$ ; R = Bu, Oct, Dod) on the micelle formation of CTAB by the tensiometric method showed that the addition of calixarenes in a concentration of  $1 \cdot 10^{-4} \text{ mol L}^{-1}$  changed substantially the shape of the surface tension ( $\sigma$ ) isotherm of CTAB (Fig. 1) and resulted in the first plateau in the concentration region from  $1.0 \cdot 10^{-4}$  to  $3.0 \cdot 10^{-4} \text{ mol L}^{-1}$ . With an increase in the CTAB content, the first plateau is changed by the region of higher values of the surface tension in solutions, whereas at the concentration  $1.0 \cdot 10^{-3} \text{ mol L}^{-1}$ ,

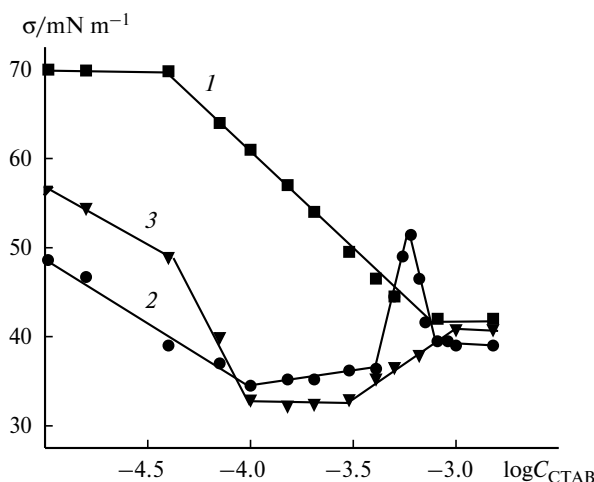


**Fig. 1.** Plots of the surface tension ( $\sigma$ ) of aqueous solutions of CTAB vs concentration in the absence (1) and in the presence of SCA 1 (2) and 3 (3) ( $C_1 = C_3 = 1.0 \cdot 10^{-4} \text{ mol L}^{-1}$ ).

which almost coincides with the CMC ( $8.0 \cdot 10^{-4} \text{ mol L}^{-1}$ ), the isotherm reaches the second plateau. The surface tension of the mixed systems in the region of the first plateau decreases to 33–35  $\text{mN m}^{-1}$ , which is lower than the  $\sigma$  value in the CMC point of individual (see Fig. 1, curve 1; also see literature data<sup>8</sup>) and mixed (see Fig. 1, curves 2 and 3) solutions of CTAB and SCA 1 and 3. An analogous run of the plot of the surface tension of aqueous solutions of CTAB has been described<sup>16</sup> for the mixed system containing water-soluble octasubstituted calix[4]resorcinarene with tris(hydroxymethyl)methylamide fragments in addition to CTAB. The shape of the surface tension isotherms for the 1–CTAB and 2–CTAB systems is identical (see Fig. 1, curve 2) but somewhat differs from the isotherm for the 3–CTAB system (see Fig. 1, curve 3). According to the published data,<sup>8</sup> micelle formation in aqueous solutions of SCA 3 has a more complicated stepped character than that in solutions of SCA 1 and 2, which can be a reason for difference in self-organization processes of mixed systems based on these SCA.

The study of CTAB solutions ( $C_{\text{CTAB}} = 1.0 \cdot 10^{-5} - 1.0 \cdot 10^{-3} \text{ mol L}^{-1}$ ) and mixtures 1–CTAB and 3–CTAB ( $C_1 = C_3 = 1.0 \cdot 10^{-4} \text{ mol L}^{-1}$ ) by the dynamic light scattering method showed that nanoparticles are formed in individual (CTAB) and mixed SCA–CTAB solutions. The solutions are characterized by the bi- or monomodal polydisperse particle size distribution. The polydispersity index is 0.1–0.3, which makes it possible to describe the totality of particle sizes in the real system using the averaged diameter ( $D$ ) at the maximum of the curve of the particle size distribution.

In micelle concentration ranges of  $1.0 \cdot 10^{-3}$  and  $1.0 \cdot 10^{-2} \text{ mol L}^{-1}$  the CTAB solutions are characterized by the bimodal particle size distribution. At the CTAB concentration  $1.0 \cdot 10^{-2} \text{ mol L}^{-1}$  the solution contains 85% of particles 4 nm in size and 15% of particles 200 nm in size, whereas at  $C_{\text{CTAB}} = 1.0 \cdot 10^{-3} \text{ mol L}^{-1}$  the solution contains approximately equal amounts of particles with sizes of 2 and 170 nm. The further dilution of CTAB solutions results in the situation when at its concentrations below the CMC ( $8.0 \cdot 10^{-4} \text{ mol L}^{-1}$ ) the solutions contain only particles with a size of 100–260 nm. Particles 2 and 4 nm in size found in the micellar region represent CTAB micelles, which agrees well with the literature data.<sup>22</sup> As for nanoparticles with a size of an order of hundreds of nanometers, it is most probable that they are similar in nature to supramolecular structures (giant clusters) described recently<sup>23,24</sup> and to nanoassociates, which have been found for the first time in solutions of low concentrations.<sup>25–27</sup> The authors of these works assume that ordered structures of water along with molecules or ions of the solute participate in the formation of such associates. The plot of the nanoassociate sizes vs CTAB concentration in the interval below  $10^{-5} \text{ mol L}^{-1}$  is shown in Fig. 2 (curve 1).

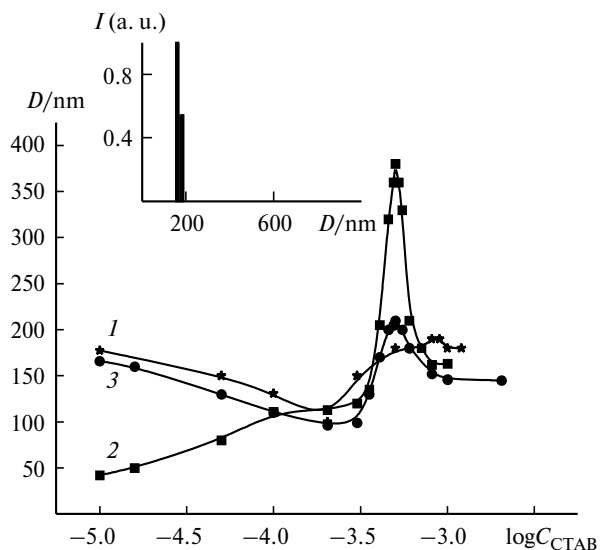


**Fig. 2.** Plots of the effective hydrodynamic diameter ( $D$ ) of nanoparticles in a solution of CTAB (1) and systems 1—CTAB (2) and 3—CTAB (3) vs CTAB concentration ( $C_1 = C_3 = 1.0 \cdot 10^{-4} \text{ mol L}^{-1}$ ). Inset: particle size distribution in a 3—CTAB solution ( $C_{\text{CTAB}} = 1.0 \cdot 10^{-6} \text{ mol L}^{-1}$ ,  $C_3 = 1.0 \cdot 10^{-4} \text{ mol L}^{-1}$ ).

A comparison of the plots  $\sigma = f(C_{\text{CTAB}})$  (see Fig. 1, curve 1) and  $D = f(C_{\text{CTAB}})$  (see Fig. 2, curve 1) indicates that the decrease in the surface tension in individual CTAB solutions in the concentration interval from  $10^{-2}$  to  $10^{-5} \text{ mol L}^{-1}$  is related to the formation of micelles in the solution, and the formation and rearrangement of nanoassociates in the pre-micellar concentration range exert almost no effect on the  $\sigma$  values of the solutions.

In mixed systems 1—CTAB and 3—CTAB in the whole studied concentration interval, the particle size concentration is almost monomodal and the solution contain mainly nanoparticles, whose sizes are hundreds of nanometers (see Fig. 2, curves 2 and 3). The particle size distribution in a 3—CTAB solution is exemplified in inset in Fig. 2.

In 1—CTAB and 3—CTAB systems, the concentration plots of the nanoparticle sizes (see Fig. 2) and the surface tension isotherms of solutions (see Fig. 1) change in parallel: the concentration ranges in which the  $D$  and  $\sigma$  values change and the intervals containing almost no changes (plateaus) coincide completely. This indicates that the formation and rearrangement of nanoparticles result first in the change in the surface tension of solutions. The appearance of the plateaus in the plots  $D = f(C_{\text{CTAB}})$  and  $\sigma = f(C_{\text{CTAB}})$  in the CMC region ( $1.0 \cdot 10^{-3} \text{ mol L}^{-1}$ ) (see Figs 1 and 2) is evidently related to the formation of mixed vermiciform micelles SCA—CTAB (SCA = 1—3) 150—160 nm in size. Another plateau in the region of comparable concentrations of CTAB ( $1.0 \cdot 10^{-4}$ — $3.0 \cdot 10^{-4} \text{ mol L}^{-1}$ ) and SCA 1—3 ( $1.0 \cdot 10^{-4} \text{ mol L}^{-1}$ ) at the component ratio (1 : 1)—(1 : 3) is due to the formation of mixed particles with the size about 100 nm in the solution. These particles

have a higher surface activity than mixed SCA—CTAB micelles and micelles of individual CTAB and SCA 1—3 (see Ref. 8). The routes of formation of such particles remain yet unclear. Taking into account the ratios of components CTAB—tetrameric SCA and the particle sizes in mixed and individual systems, one can believe that intermolecular complexes formed primarily due to the sulfonate groups of calixarene and the ammonium group of CTAB involving the alkyl radicals of both components represent a structural unit of mixed particles. These complexes should be more hydrophobic than the starting components and, therefore, should manifest a higher surface activity. Considerable sizes of the particles detected in the plateau region ( $C_{\text{CTAB}} \approx 1.0 \cdot 10^{-4} \text{ mol L}^{-1}$ ) can be due to either aggregation of the complexes, or the formation of nanoassociates formed by intermolecular complexes and structures of water analogously to the process described earlier.<sup>24</sup> An increase in  $C_{\text{CTAB}}$  results in the rearrangement of particles and formation of micellar ensembles in the region of high CTAB concentrations.

The interaction of nanoassociates of CTAB and SCA 3 depends substantially on the concentration of the latter, *i.e.*, on the state in which the added substance exists in solution.<sup>8</sup> The shape of the surface tension isotherms changes substantially upon the change in the concentration of SCA 3 in a mixed system from  $2.0 \cdot 10^{-5}$  to  $2.0 \cdot 10^{-4} \text{ mol L}^{-1}$ . In the former case ( $2.0 \cdot 10^{-5} \text{ mol L}^{-1}$ ), the isotherm is analogous to those for the systems shown in Fig. 1 (curve 3). In the latter case, the isotherm is similar to the isotherms of mixed micellar systems with one CMC ( $2.0 \cdot 10^{-4} \text{ mol L}^{-1}$ ), which is by 4 times lower than the CMC of cetyltrimethylammonium bromide.

Thus, the systems based on CTAB and SCA 3 in the concentration range from  $2.0 \cdot 10^{-5}$  to  $2.0 \cdot 10^{-4} \text{ mol L}^{-1}$  exhibit the formation of mixed nanoparticles and a decrease in the surface tension of the solutions in the pre-micellar region of CTAB concentrations ( $1.0 \cdot 10^{-4}$ — $3.0 \cdot 10^{-4} \text{ mol L}^{-1}$ ) to 33—35 mN  $\text{m}^{-1}$ , which is lower than the  $\sigma$  value in CTAB solutions with a micellar concentration ( $8.0 \cdot 10^{-4} \text{ mol L}^{-1}$ ).

To study the influence of the size of the calixarene macrocycle and of the concentrations of components of the mixture on self-organization in CTAB—SCA systems, we examined the concentration dependences of the surface tension of CTAB solutions ( $1.0 \cdot 10^{-18}$ — $1.0 \cdot 10^{-2} \text{ mol L}^{-1}$ ) in the presence of hexameric SCA 4 ( $n = 6$ ,  $R = \text{Dod}$ ), whose concentration was varied from  $1.0 \cdot 10^{-6}$  to  $2.5 \cdot 10^{-4} \text{ mol L}^{-1}$ . In aqueous solutions in a wide concentration range compound 4 forms nanoparticles, whose size is 200—250 nm.<sup>8</sup> As in solutions of SCA 3, the micelle formation process in aqueous solutions of SCA 4 has a stepped character in the concentration range from  $1.0 \cdot 10^{-4}$  to  $6.0 \cdot 10^{-4} \text{ mol L}^{-1}$ .

The surface tension isotherms of CTAB solutions (the region of changing the CTAB concentration is

$1.0 \cdot 10^{-6}$ – $1.0 \cdot 10^{-2}$  mol L $^{-1}$ ) in the presence of SCA **4** ( $1 \cdot 10^{-4}$  mol L $^{-1}$ ) at low CTAB concentrations have a more complicated shape than in the presence of SCA **1**–**3**, whereas the CMC of the mixed system remains almost unchanged, being  $8 \cdot 10^{-4}$  mol L $^{-1}$  (Fig. 3). A comparison of the concentration plots  $\sigma = f(C_{\text{CTAB}})$  and  $D = f(C_{\text{CTAB}})$  presented in Fig. 3 shows that the  $\sigma$  value in a **4**–CTAB solution changes in parallel with the nanoparticle size. As in the case of SCA–CTAB mixed systems (SCA = **1**–**3**), a decrease in the surface tension in the pre-micellar concentration range is due to the formation of mixed nanoparticles and their structural rearrangements. The plots  $\sigma = f(C_{\text{CTAB}})$  and  $D = f(C_{\text{CTAB}})$  in a **4**–CTAB system differ substantially from similar dependences for solutions of individual CTAB (see Figs 1 and 3). Note that, unlike all previous systems studied, in this case, the  $\sigma$  value turned out to be very low in the initial points of the concentration dependence  $\sigma = f(C_{\text{CTAB}})$ . For instance, at  $C_{\text{CTAB}} = 2 \cdot 10^{-5}$  mol L $^{-1}$  the  $\sigma$  value of the system is 45 mN m $^{-1}$ . This surface tension is characteristic of many surfactants and mixed systems in the range of CMC.<sup>13</sup> As it has been shown earlier,<sup>8</sup> the concentration of SCA **4** equal to  $1.0 \cdot 10^{-4}$  mol L $^{-1}$  induces a decrease in  $\sigma$  of solutions of compound **4** only to 60 mN m $^{-1}$ , whereas CTAB in a concentration of  $2.0 \cdot 10^{-5}$  mol L $^{-1}$  does not almost decrease the surface tension of aqueous solutions (see Fig. 1). As can be seen from Fig. 3, the decrease in the surface tension of a mixed solution at  $C_{\text{CTAB}} = 2.0 \cdot 10^{-5}$  mol L $^{-1}$  and  $C_4 = 1.0 \cdot 10^{-4}$  mol L $^{-1}$  is related to the formation of **4**–CTAB nanoparticles 160 nm in size.

To determine the optimum concentrations of CTAB and SCA **4** at which nanosized particles manifesting high surface activity can be formed, we obtained the surface tension isotherms of solutions of CTAB and a **4**–CTAB

system in a broader range of the CTAB concentrations: down to  $10^{-18}$  mol L $^{-1}$  (Fig. 4). The concentrations of SCA **4** in a mixture were  $5.0 \cdot 10^{-6}$ ,  $1.0 \cdot 10^{-5}$ ,  $2.0 \cdot 10^{-5}$ ,  $6.0 \cdot 10^{-5}$ ,  $1.0 \cdot 10^{-4}$ , and  $2.5 \cdot 10^{-4}$  mol L $^{-1}$ . The addition of compound **4** in concentrations of  $5.0 \cdot 10^{-6}$ – $2.0 \cdot 10^{-5}$  mol L $^{-1}$  induced no substantial change in the shape of the isotherms of a CTAB solution. An increase in the concentration of SCA **4** in a mixed system to  $6.0 \cdot 10^{-5}$ – $2.5 \cdot 10^{-4}$  mol L $^{-1}$  results in a considerable decrease in the  $\sigma$  value (45–50 mN m $^{-1}$ ) almost in the whole range of CTAB concentrations down to  $10^{-12}$  mol L $^{-1}$  (see Fig. 4). The further decrease in the CTAB concentration (from  $10^{-12}$  to  $10^{-18}$  mol L $^{-1}$ ) is accompanied by an increase in the  $\sigma$  values in the system; at  $C_{\text{CTAB}} = 10^{-16}$  mol L $^{-1}$  the  $\sigma$  value reaches the level corresponding to the surface tension of solutions of individual SCA **4** at the concentrations  $6.0 \cdot 10^{-5}$ ,  $1.0 \cdot 10^{-4}$ , and  $2.5 \cdot 10^{-4}$  mol L $^{-1}$  (curves 2–4, respectively).<sup>8</sup>

The dynamic light scattering method showed that in a mixed solution at low CTAB concentrations ( $10^{-5}$ – $10^{-18}$  mol L $^{-1}$ ) associates with the accumulation fraction  $\sim 0.99$  were formed. A comparison of the concentration plots of the surface tension (see Fig. 3, curve 3; Fig. 4; Fig. 5, curve 3) and the sizes of the associates (see Fig. 3, curve 2; Fig. 5, curve 2) indicates the resemblance of the concentration ranges in which the  $\sigma = f(C_{\text{CTAB}})$  and  $D = f(C_{\text{CTAB}})$  plots undergo the most significant changes in the surface tension and particle sizes. This suggests that mixed nanosized particles with high surface activity are responsible for the change in the  $\sigma$  value of solutions in the range of CTAB concentrations from  $10^{-12}$  to  $10^{-7}$  mol L $^{-1}$ . At the CTAB concentrations lower than  $10^{-12}$  mol L $^{-1}$ , particles with a size of  $\sim 240$  nm are formed in the solution, which corresponds to the size of individual nanoparticles of SCA **4**. Taking into account very low CTAB con-

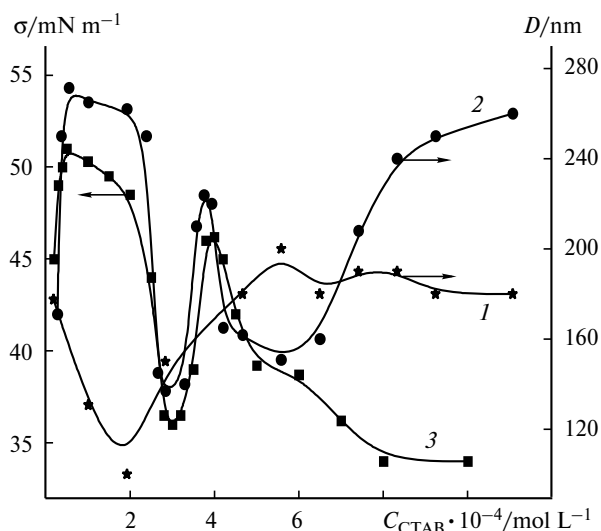


Fig. 3. Plots of the particle size (1, 2) and surface tension (3) vs CTAB concentration in the absence (1) and in the presence (2, 3) of SCA **4** ( $C_4 = 1.0 \cdot 10^{-4}$  mol L $^{-1}$ ).

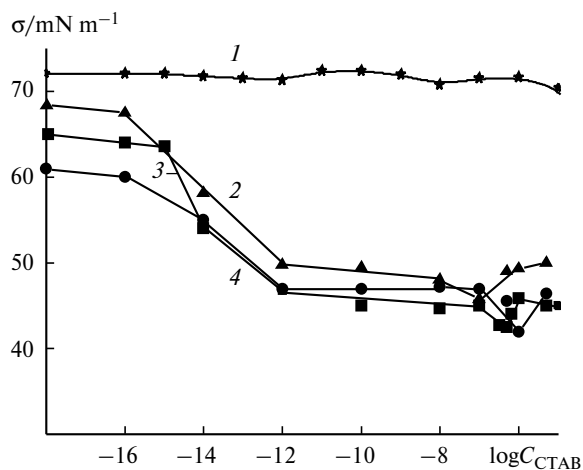
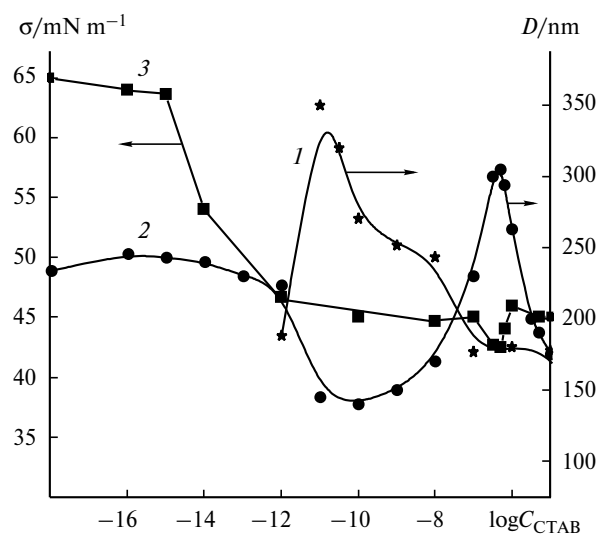


Fig. 4. Plots of the surface tension of aqueous CTAB solutions vs concentration in the absence (1) and in the presence of SCA **4** additives in a concentration of  $6.0 \cdot 10^{-5}$  (2),  $1.0 \cdot 10^{-4}$  (3), and  $2.5 \cdot 10^{-4}$  mol L $^{-1}$  (4).



**Fig. 5.** Plots of the sizes of associates (1, 2) and surface tension (3) vs CTAB concentration in the absence (1) and in the presence (2, 3) of SCA 4 ( $C_4 = 1.0 \cdot 10^{-4} \text{ mol L}^{-1}$ ) in the region of low and superlow concentrations.

centrations, considerable sizes of the mixed particles, and the fact that the observed significant decrease in the surface tension of mixed solutions needs concentrations of SCA 4 at which nanoparticles are rearranged and the  $\sigma$  values of individual solutions of SCA 4 decrease,<sup>8</sup> it is reasonable to assume that associates of SCA 4 play a substantial role in the formation of mixed nanoparticles in a 4–CTAB system in the region of low CTAB concentrations. At the same time, it remains unclear why such a powerful synergic effect of the mixed system is observed only in a certain range of CTAB concentrations (over  $10^{-12} \text{ mol L}^{-1}$ ). (In the works devoted to the study of biologically active substances in the low and superlow concentrations, the concentrations lower than  $10^{-12} \text{ mol L}^{-1}$  are named superlow or "imaginary"; see Ref. 28).

We have earlier shown<sup>27</sup> for the first time that in individual CTAB solutions nanoassociates are formed down to a concentration of  $10^{-10} \text{ mol L}^{-1}$ . It is established that the rearrangement of nanoassociates is responsible for the nonlinear change in some physicochemical properties of solutions in the region of low and superlow concentrations, primarily for the appearance of the nonlinear concentration dependences of the specific electroconductivity of solutions.<sup>25,26</sup> To reveal the role that can be played by CTAB nanoassociates in the formation of mixed 4–CTAB nanoparticles, we studied the dependences  $\sigma = f(C_{\text{CTAB}})$  and  $D = f(C_{\text{CTAB}})$  down to  $C_{\text{CTAB}} = 10^{-16} \text{ mol L}^{-1}$ . We managed to detect reliably the sizes of CTAB particles to the value  $C_{\text{CTAB}} = 10^{-12} \text{ mol L}^{-1}$ . The data on the size of the nanoassociates formed in individual solutions of CTAB are shown in Fig. 5 (curve 1). Note that in individual solutions of CTAB at the concentrations lower than

$10^{-12} \text{ mol L}^{-1}$  the specific electroconductivity decreases, while it remains unchanged in the range from  $10^{-14}$  to  $10^{-18} \text{ mol L}^{-1}$  and almost corresponds to the electric conductivity of bidistilled water. With allowance for these data it becomes evident that the  $\sigma$  values of the solutions and the sizes of associates in the mixed system reach the level corresponding to solutions of individual SCA 4 at the CTAB concentrations lower than  $10^{-12} \text{ mol L}^{-1}$ , because nanoparticles of the second component (CTAB) are absent in this range of concentrations in this solution. The run of the  $\sigma = f(C_{\text{CTAB}})$  and  $D = f(C_{\text{CTAB}})$  plots in 4–CTAB solutions with an increase in the CTAB concentration can be interpreted as follows. In the range  $C_{\text{CTAB}} = 10^{-14}–10^{-18} \text{ mol L}^{-1}$ , particles of SCA 4 exist in the solution bulk, and then surfactant associates are formed in the range  $10^{-12}–10^{-7} \text{ mol L}^{-1}$  due to the interaction of particles of SCA 4 and nanoassociates of CTAB. These associates undergo considerable rearrangements with an increase in the CTAB concentration. In an excess of CTAB, mixed layers can be formed at the interface and mixed micelles are formed in the solution. It will be shown below that the mixed micelles differ in reactivity from micelles of SCA<sup>8</sup> and CTAB.

Thus, the data obtained indicate that the interaction of associates of SCA 4 and CTAB in the low region of CTAB concentrations ( $10^{-12}–10^{-7} \text{ mol L}^{-1}$ ) results in the spontaneous formation of mixed nanoparticles with a size of 140–200 nm, the latter efficiently decreasing the surface tension of aqueous mixed solutions. The supramolecular system 4–CTAB demonstrates a possibility of substantial changes in the physicochemical properties of solutions due to the interactions of associates of dissolved substances formed in the region of nanoconcentrations of the components. The shape of the concentration plots of the  $\sigma$  and  $D$  values for a 4–CTAB system in the range of CTAB concentrations from  $10^{-12}$  to  $10^{-5} \text{ mol L}^{-1}$  is analogous to that of the nonmonotonic concentrations plots of the bio-effects<sup>28</sup> and physicochemical properties of solutions<sup>25–27</sup> of biologically active substances in the range of low and superlow concentrations. This makes it possible to consider associates of SCA 4 as a convenient biomimetic supramolecular system for studying the self-organization of biologically active substances in the range of low and superlow concentrations.

In the case of octameric SCA 5 ( $n = 8$ ,  $R = \text{Dod}$ ), the interaction with CTAB is much less efficient. The surface tension isotherm contains the inflection point at  $5 \cdot 10^{-4} \text{ mol L}^{-1}$ , and the CMC of the system ( $8 \cdot 10^{-4} \text{ mol L}^{-1}$ ) coincides with the CMC of cetyltrimethylammonium bromide.

To study the catalytic activity of mixed systems based on alkylated SCA and CTAB, we analyzed the kinetics of the hydrolysis of ENCP (Figs 6 and 7) in aqueous mixed solutions of CTAB and SCA 3–5 by the spectrophotometric method.

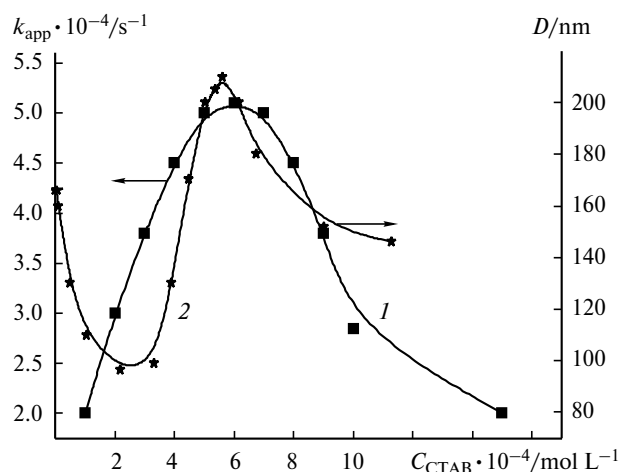


**Fig. 6.** Plots of the apparent reaction rate constant (1) of hydrolysis of ENCP and of the particle size (2) vs CTAB concentration in an aqueous solution of the 3-CTAB system ( $C_3 = 1.0 \cdot 10^{-4} \text{ mol L}^{-1}$ , pH 8, 25 °C).

The nonlinear profile of the plot  $k_{\text{app}} = f(C_{\text{CTAB}})$  with a pronounced maximum is observed in the systems based on CTAB and SCA 3 and 5, whereas in the system based on CTAB and SCA 4 the observed plot reaches a plateau. Both types of kinetic curves are characteristic of micelle-catalyzed reactions.<sup>11</sup> The reaction parameters calculated by Eq. (1) are listed in Table 1. The rate constants of the reaction in the micellar phase ( $k_m$ ) for mixed systems are approximately equal to the corresponding rate constants in CTAB solutions or by 2–3 times lower. However, the maximum catalytic activity of the system is achieved at much lower CTAB concentrations, which reflects the high values of the binding constants of the substrates ( $K_b$ ) by mixed SCA-CTAB micelles, which are approximately 10, 25, and 70 times higher than the  $K_b$  values by CTAB

**Table 1.** Kinetic parameters of hydrolysis of *O*-ethyl *O*-(4-nitrophenyl) chloromethylphosphonate in the supramolecular systems based on CTAB and SCA ( $C_{\text{SCA}} = 1.0 \cdot 10^{-4} \text{ mol L}^{-1}$ )

System	$k_m \cdot 10^4 / \text{s}^{-1}$	$K_b / \text{L mol}^{-1}$	$\text{CMC} \cdot 10^4 / \text{mol L}^{-1}$
CTAB	13.0	370	6.1
CTAB-3	5.2	3100	1.3
CTAB-4	11.0	8000	1.8
CTAB-5	8.0	25000	7.8

for SCA 3, 4, and 5, respectively. The binding constants of the substrate increase with an increase in the size and conformational mobility of the macrocycle, resulting in the appearance of the adaptive ability to bind the substrate (flexible tuning) by SCA molecules<sup>29</sup> and also by their mixed micellar aggregates.

Different assumptions on reasons for the appearance of the extreme kinetic dependences are advanced in the literature: for example, the retardation of the reaction with an increase in the surfactant concentration is attributed to the dilution of the reactants in the micellar phase.<sup>11</sup> In the reactions considered, the "extreme" profiles of the  $k_{\text{app}} = f(C_{\text{CTAB}})$  plots are due, most probably, to the change in the structure and reactivity of mixed aggregates SCA-CTAB. To confirm this assumption, we used the dynamic light scattering method to study the effect of the CTAB concentration on the effective diameters of mixed SCA-CTAB micelles under the conditions identical to those used in the kinetic study (see Figs 6 and 7). As can be seen, an increase in the CTAB content in the SCA-CTAB systems leads to an increase in the sizes of the mixed aggregates and an enhancement of their catalytic activity. The further increase in the CTAB concentration in the systems CTAB-SCA 3 and 5 is accompanied by the parallel decrease in their catalytic activity and a decrease in the sizes of mixed aggregates, whereas in the 4-CTAB system the both dependences reach a plateau. Thus, the catalytic activity of supramolecular systems SCA-CTAB is associated with the formation and structural rearrangement of mixed aggregates, *i.e.*, with a certain structure of supramolecular nanoparticles based on amphiphilic SCA and CTAB.

We have previously shown<sup>8</sup> that the most pronounced membrane-active properties are manifested by hexameric and octameric *p*-sulfonatocalixarenes 4 and 5 modified by dodecyl radicals, which substantially stimulate or suppress the energy exchange in wheat root cells. In addition, in the present work a unique ability of SCA 4 associates was found: they can form mixed aggregates with CTAB nanoassociates down to  $C_{\text{CTAB}} = 10^{-12} \text{ mol L}^{-1}$ . That is why we studied the effect of the supramolecular systems based on CTAB and SCA for solutions of SCA 4 in a concentration of  $5.0 \cdot 10^{-5} \text{ mol L}^{-1}$ .

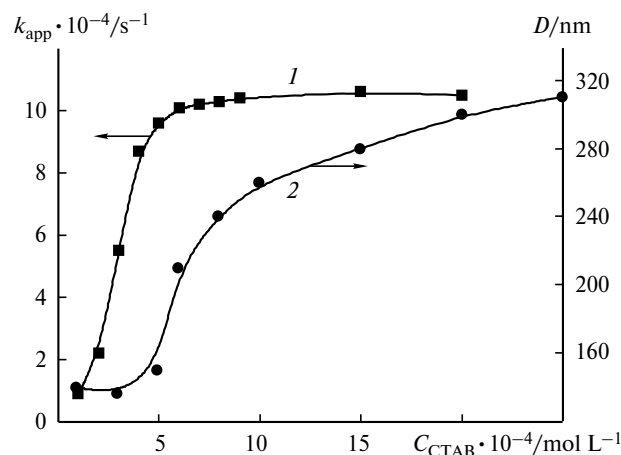


**Fig. 7.** Plots of the apparent reaction rate constant (1) of hydrolysis of ENCP and of the particle size (2) vs CTAB concentration in an aqueous solution of the 4-CTAB system ( $C_4 = 1.0 \cdot 10^{-4} \text{ mol L}^{-1}$ , pH 8, 25 °C).

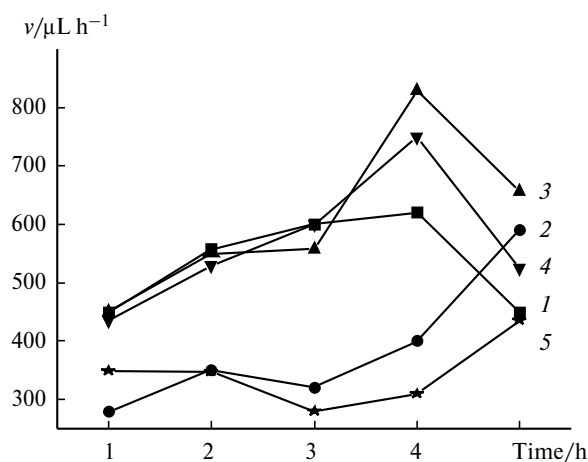


**Fig. 8.** Dynamics of oxygen consumption ( $v$ ) by wheat roots in reference experiments (1) under the action of solutions of CTAB (2) and SCA 4 (3) and mixed solutions 4—CTAB (4, 5) ( $C_{\text{CTAB}} = 5.0 \cdot 10^{-5}$  (2, 4),  $2.5 \cdot 10^{-4}$  mol L $^{-1}$  (5);  $C_4 = 5.0 \cdot 10^{-5}$  mol L $^{-1}$ ).

It is known that the cationic surfactants have biological activity and their interaction with biological structures results in cell damage, leading to its decay.<sup>10</sup> It was also found that the cationic surfactants favor the deorganization of the cell membrane and denaturation of indispensable cell enzymes.<sup>10</sup> The study of the physiological action on the plant cells of SCA 4 and CTAB showed that these substances in a concentration of  $5.0 \cdot 10^{-5}$  mol L $^{-1}$  exert a noticeable effect, but with opposite directions, on oxygen consumption by the roots, the pH value of the incubation medium, and the escape of potassium ions from the cells: SCA 4 stimulates the energy exchange of the cut-off wheat roots, whereas CTAB suppresses the latter (Fig. 8). As it was shown by the study of the physiological behavior of the CTAB—4 system, the interaction of SCA and CTAB under biological conditions can result in the almost complete elimination of the effect of these substances on the cell membrane, which is due to the formation of stable mixed aggregates CTAB—4 protecting the biomembrane from the action of the starting components. A mixed solution containing CTAB in a higher concentration ( $2.5 \cdot 10^{-4}$  mol L $^{-1}$ ), which fivefold exceeds the concentration of SCA 4, does not completely align the effect of CTAB but makes it considerably less pronounced. Thus, we showed that the associates of SCA 4 formed in the region of pre-micellar concentrations are capable of strong binding the CTAB nanoassociates in both aqueous solutions and biosystems to form mixed associates, which exert almost no effect on the physiological state of plant cells.

This work was financially supported by the Russian Foundation for Basic Research (Project Nos 06-03-32402 and 10-03-00147).

## References

1. *Calixarenes 2001*, Eds Z. Asfari, V. Bohmer, J. Harrowfield, J. Vicens, Kluwer Academic Publishers, Dordrecht—Boston—London, 2001, 683.
2. *Calixarenes in Action*, Eds L. Mandolini, R. Ungaro, Imperial College Press, London, 2000, 271.
3. J. W. Steed, J. L. Atwood, *Supramolecular Chemistry*, J. Wiley and Sons, New York—London, 2000.
4. Dong-Sheng Guo, Kui Wang, Yu Liu, *J. Incl. Phenom. Macromol. Chem.*, 2008, **62**, 1.
5. F. Perret, A. N. Lazar, A. W. Coleman, *Chem. Commun.*, 2006, 2425.
6. T. Ogoshi, T. Yamagishi, Y. Nakamoto, *Chem. Commun.*, 2007, 4776.
7. A. S. Lobach, I. S. Ryzhkina, N. G. Spitsina, E. D. Obratsova, *Phys. Stat. Sol. B*, 2007, **244**, 4030.
8. I. S. Ryzhkina, Yu. V. Kiseleva, S. E. Solov'eva, L. M. Pilishkina, Yu. N. Valitova, A. I. Konovalov, *Izv. Akad. Nauk, Ser. Khim.*, 2009, 2424 [*Russ. Chem. Bull., Int. Ed.*, 2009, **58**, 2506].
9. Chun Liu, Zhong Fu, Huapeng Yu, Hongwei Xu, Lun Wang, Yunyou Zhou, *J. Luminescence*, 2007, 747.
10. E. F. Gale, E. Cundliffe, P. E. Reynolds, M. H. Richmond, M. Waring, *The Molecular Basis of Antibiotic Action*, Wiley-Interscience Publ., J. Wiley and Sons, New York—London, 1972.
11. E. P. Tishkova, L. A. Kudryavtseva, *Izv. Akad. Nauk, Ser. Khim.*, 1996, 298 [*Russ. Chem. Bull. (Engl. Transl.)*, 1996, **45**, 284].
12. S. B. Savvin, R. K. Chernova, S. N. Shtykov, *Poverkhnostno-aktivnye veshchestva [Surfactants]*, Nauka, Moscow, 1991, 251 pp. (in Russian).
13. K. Holmberg, B. Jonsson, B. Kronberg, B. Lindman, *Surfactants and Polymers in Aqueous Solutions*, 2nd ed., J. Wiley and Sons, New York—London, 2003.
14. I. S. Ryzhkina, L. A. Kudryavtseva, Ya. A. Babkina, K. M. Enikeev, M. A. Pudovik, A. I. Konovalov, *Izv. Akad. Nauk, Ser. Khim.*, 2000, 1361 [*Russ. Chem. Bull., Int. Ed.*, 2000, **49**, 1355].
15. I. S. Ryzhkina, T. N. Pashirova, Ya. A. Filippova, L. A. Kudryavtseva, A. P. Timosheva, V. P. Arkhipov, Z. Sh. Idiyatullin, E. V. Popova, A. R. Burilov, A. I. Konovalov, *Izv. Akad. Nauk, Ser. Khim.*, 2004, 1462 [*Russ. Chem. Bull., Int. Ed.*, 2004, **53**, 1520].
16. I. S. Ryzhkina, T. N. Pashirova, W. D. Habicher, L. A. Kudryavtseva, A. I. Konovalov, in *Macromolecular Symposia: Reactive Polymers 2003 (Dresden, Germany, 2003)*, Ed. H.-J. P. Adler, Wiley—VCH Verlag GmbH and Co., 2004, 41.
17. I. S. Ryzhkina, T. N. Pashirova, S. S. Lukashenko, A. P. Timosheva, Yu. I. Sal'nikov, G. A. Boos, L. A. Kudryavtseva, A. I. Konovalov, *Zhidkie kristally i ikh prakticheskoe ispol'zovanie [Liquid Crystals and Their Practical Use]*, 2004, issue 1, 69 (in Russian).
18. C. D. Gutsche, I. Alam, *Tetrahedron*, 1988, **44**, 4689.
19. M. Komiyama, K. Isaka, S. Shinkai, *Chem. Lett.*, 1991, 937.
20. J. L. Atwood, D. L. Clark, R. K. Juneja, G. W. Orr, K. D. Robinson, R. L. Vincent, *J. Am. Chem. Soc.*, 1992, **114**, 7558.
21. I. S. Ryzhkina, V. D. Khabikher, Yu. V. Kiseleva, A. P. Timosheva, A. I. Konovalov, Yu. N. Valitova, G. N. Mar-



- danova, A. N. Tsentskevitskii, L. Kh. Gordon, *Dokl. Akad. Nauk*, 2007, **413**, 557 [*Dokl. Chem. (Engl. Transl.)*, 2007, **413**, 68].
22. S. De, V. R. Aswal, P. S. Goel, S. Bhattacharya, *J. Phys. Chem. B*, 1997, **101**, 5639.
23. M. Sedlak, *J. Phys. Chem. B*, 2006, **110**, 4329.
24. G. V. Andrievsky, V. I. Bruskov, A. A. Tykhomyrov, S. V. Gudkov, *Free Radical Biol. Med.*, 2009, **47**, 786.
25. A. I. Kononov, I. S. Ryzhkina, L. I. Murtazina, A. P. Timosheva, R. R. Shagidullin, A. V. Chernova, L. V. Avvakumova, S. G. Fattakhov, *Izv. Akad. Nauk, Ser. Khim.*, 2008, 1207 [*Russ. Chem. Bull., Int. Ed.*, 2008, **57**, 1231].
26. I. S. Ryzhkina, L. I. Murtazina, Yu. V. Kiseleva, A. I. Kononov, *Dokl. Akad. Nauk*, 2009, **428**, 487 [*Dokl. Chem. (Engl. Transl.)*, 2009, **428**].
27. I. S. Ryzhkina, L. I. Murtazina, Yu. V. Kiseleva, A. I. Kononov, *Dokl. Akad. Nauk*, 2009, **428**, 628 [*Dokl. Chem. (Engl. Transl.)*, 2009, **428**].
28. E. B. Burlakova, *Ros. Khim. Zh. (Zh. Ros. Khim. Obshch. im. D. I. Mendeleeva)*, 2007, No. 1, 3 [*Mendeleev Chem. J. (Engl. Transl.)*, 2007, No. 1].
29. A. Specht, Ph. Bernard, M. Goldner, L. Peng, *Angew. Chem., Int. Ed. Engl.*, 2002, **41**, 4706.

Received November 25, 2008;  
in revised form April 25, 2010